

Figure 11 are detectable in electron transmission spectroscopy. However, the proximity of the observed optical absorption bands at about 3.5 eV to the $\bar{B} \leftarrow \bar{X}$ transitions seems to indicate a correspondence. The broadness of the resolved bands in Figure 11 is reminiscent of a similar bandshape of benzene anion and recalls the ease of the electron detachment of optically excited anions.^{5c,20}

Note Added in Proof. The cation radical of pyridine has been recently identified to be a σ cation (see Shida, T.; Kato, T. *Chem. Phys. Lett.*, in press).

Acknowledgments. The authors wish to thank Dr. Masashi Imamura, who allowed them to use the facilities at the Institute of Physical and Chemical Research. They acknowledge also Dr. Yoshio Nosaka for his help in the ESR measurement at 4 K.

References and Notes

- (1) (a) Goodman, L. *J. Mol. Spectrosc.* **1961**, *6*, 109–137. (b) Innes, K. K.; Byrne, J. P.; Ross, I. G. *Ibid.* **1967**, *22*, 125–147.
- (2) McGlynn, S. P.; Azumi, T.; Kinoshita, M. "Molecular Spectroscopy of the Triplet State", Prentice-Hall: Englewood Cliffs, N.J., 1969.
- (3) Gerson, F. "High Resolution ESR Spectroscopy", Wiley, New York, 1970.
- (4) Siegbahn, K. In "Handbook of Spectroscopy", Robinson, J. W., Ed.; CRC Press: Cleveland, 1974; Vol. 1.

- (5) (a) Shida, T.; Iwata, S. *J. Phys. Chem.* **1971**, *75*, 2591–2602. (b) *J. Chem. Phys.* **1972**, *56*, 2858–2864. (c) *J. Am. Chem. Soc.* **1973**, *95*, 3473–3483. (d) Shida, T.; Iwata, S.; Imamura, M. *J. Phys. Chem.* **1974**, *78*, 741–749.
- (6) Shida, T.; Nosaka, Y.; Kato, T. *J. Phys. Chem.* **1977**, *81*, 1095–1103.
- (7) Kasai, P. H.; Hedayat, E.; Whipple, E. B. *J. Am. Chem. Soc.* **1969**, *91*, 4364–4368.
- (8) (a) Gleiter, R.; Heilbronner, E.; Hornung, V. *Helv. Chim. Acta* **1972**, *55*, 255–274. (b) Brogli, F.; Heilbronner, E.; Kobayashi, T. *Ibid.* **1972**, *55*, 274–288.
- (9) Hush, N. S.; Cheung, A. S.; Hilton, P. R. *J. Electron Spectrosc. Relat. Phenom.* **1975**, *7*, 385–400.
- (10) Shida, T. *J. Phys. Chem.* **1969**, *73*, 4311–4314.
- (11) Shida, T.; Nosaka, Y.; Kato, T. *J. Phys. Chem.* **1978**, *82*, 695–698.
- (12) Edlund, O.; Lund, A.; Shiotani, M.; Sohma, J.; Thuomas, K. A. *Mol. Phys.* **1976**, *32*, 49–69.
- (13) Hoffmann, R.; Imamura, A.; Hehre, M. J. *J. Am. Chem. Soc.* **1968**, *90*, 1499–1509.
- (14) von Niessen, W.; Diercksen, G. H. F.; Cederbaum, L. S. *Chem. Phys.* **1975**, *10*, 345–360.
- (15) Hinchliffe, A. *J. Electron Spectrosc. Relat. Phenom.* **1977**, *10*, 415–422.
- (16) Scrocco, M.; Lauro, C. D.; Califano, S. *Spectrochim. Acta* **1965**, *21*, 571–577.
- (17) Grimison, A.; Simpson, G. A. *J. Phys. Chem.* **1968**, *72*, 1776–1779.
- (18) Bowers, H. J.; McRae, J. A.; Symons, M. C. R. *J. Chem. Soc. A* **1968**, 2696–2699.
- (19) Nenner, I.; Schulz, G. J. *J. Chem. Phys.* **1975**, *62*, 1747–1758.
- (20) Watanabe, T.; Shida, T.; Iwata, S. *Chem. Phys.* **1976**, *13*, 65–72.
- (21) David, C.; Janssen, P.; Geuskens, G. *Spectrochim. Acta, Part A* **1971**, *27*, 367–376.
- (22) Chaudhuri, J.; Kume, S.; Jagur-Grodzinski, J.; Szarc, M. *J. Am. Chem. Soc.* **1968**, *90*, 6421–6425.

Model Studies of the Electronic Structure of Solid-State Beryllium Borohydride

Dennis S. Marynick

Contribution from the Department of Chemistry, The University of Texas at Arlington, Arlington, Texas 76019. Received May 31, 1979

Abstract: The electronic structure of polymeric solid-state beryllium borohydride is modeled by performing molecular orbital calculations on $(\text{BeB}_2\text{H}_8)_n$ fragments, $n = 1-6$. Comparisons of atomic charges, overlap populations, localized orbitals, and electron density indicate that the solid is best viewed as nearly ionic BeBH_4^+ and BH_4^- ions. This view is consistent with previous crystallographic and infrared work. The convergence of the calculated properties of the molecular wave function as a function of chain length is examined in detail. Fair convergence is observed for $n = 3$, while essentially complete convergence is seen at $n = 5$.

Introduction

Although the structure of beryllium borohydride in the gas phase is a subject of considerable controversy,¹⁻⁵ the solid-phase structure is known with certainty from an X-ray diffraction study.⁶ The solid state consists of one-dimensional helical polymers of alternating boron and beryllium atoms about a 4_1 crystallographic screw axis, with a BH_4 group bound to the outside of the helix at each beryllium site. Figure 1 illustrates the chemical repeat of the polymer, and Figure 2 shows a projection down the helical axis. There is a double hydrogen bridge associated with every near neighbor boron-beryllium interaction, and the hydrogen coordination about beryllium is a distorted trigonal prism. The space group is $I4_1cd$, with unit cell parameters $a = 9.1$ and $b = 13.6$ Å.

Earlier, an infrared study of the solid⁷ was interpreted in terms of the ionic solid $\text{BeBH}_4^+\text{BH}_4^-$. In fact, distances obtained from the X-ray study for $\text{Be}-\text{B}_1$ (1.92 Å), $\text{Be}-\text{B}_2$ (2.00 Å), and $\text{Be}-\text{B}_2'$ (2.00 Å) suggested that the above interpretation may be substantially correct, with B_2 , the boron within the helix, being part of a BH_4^- group and B_1 being part of a BeBH_4^+ group. Nevertheless, the helical polymeric chains

suggest some compromise between the extremes of covalency (the finite molecule) and ionicity (an infinite three-dimensional solid).

In marked contrast to the polymeric nature of the solid state, the gas phase is known^{5a,8} to exist mainly in monomeric units. Many different structures have been suggested,³ but recent electron diffraction^{5b} and infrared^{5a} work tends to favor a two-structure hypothesis, one structure being linear with triple hydrogen bridges, unequal boron-beryllium bond lengths, and C_{3v} symmetry, and the other structure probably being linear with double hydrogen bridges and D_{2d} symmetry. Recent theoretical work^{3,4} is not consistent with the suggested C_{3v} conformer, but suggests that the D_{2d} structure and a linear structure with triple hydrogen bridges and D_{3d} symmetry are competitive energetically. Neither of these structures can account for the observed dipole moment.⁹

In this paper we present a molecular orbital study of models of the solid-state beryllium borohydride polymeric chain, using fragments of from one to six monomeric units and geometrical parameters defined by the previous X-ray diffraction study.⁶ We employ molecular orbital calculations in the approximation of partial retention of diatomic differential overlap

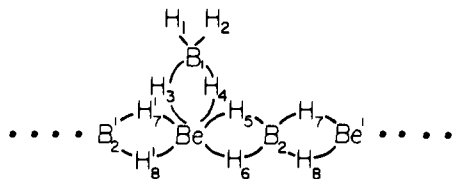


Figure 1. The chemical repeat of the beryllium borohydride polymer.

(PRDDO)¹⁰ and a minimum basis set of Slater orbitals. Various properties derived from the molecular wave functions, including total energy, inner shell eigenvalues, Mulliken charges, overlap populations, localized orbitals, and electron density, are studied as a function of chain length and compared to the monomeric gas-phase molecule. Particular emphasis is placed on two questions: is the ionic model $\text{BeBH}_4^+ \text{BH}_4^-$ an appropriate description of the solid state, and how quickly do the computed molecular properties converge to the limit of an infinite chain length? The question of the rapidity of convergence is a particularly important one, since modeling solid-state structure by relatively small clusters is an important area of current research.¹¹

Calculations

All molecular orbital calculations were done within the PRDDO approximation. This method, although more than an order of magnitude faster than ab initio calculations on moderate size molecules with the same basis set, gives results which compare very favorably with the reference ab initio calculations.¹² The PRDDO method is particularly useful for this study, since its basic n^3 dependence (rather than the n^4 dependence of ab initio methods) results in dramatic savings in computing time for the large, symmetryless systems studied here. Published¹² comparisons of PRDDO and STO-3G computing times for smaller systems suggest that an STO-3G calculation on the hexamer of beryllium borohydride (138 orbitals) would require more than two orders of magnitude more computer time than the corresponding PRDDO calculation.

All exponents were held constant at the values given by Hehre et al.¹³ Bond distances were taken as the average of the chemically equivalent distances found in the X-ray study,⁶ except for terminal B-H distances, which were set at 1.20 Å to compensate for known systematic shortening of B-H distances by X-ray diffraction.¹⁴ Other bond distances follow: $\text{B}_1\text{-H}_4$, $\text{B}_1\text{-H}_3$ (1.290 Å), Be-H_3 , Be-H_4 (1.527 Å), Be-H_5 , Be-H_6 , $\text{Be-H}_7'$, $\text{Be-H}_8'$ (1.611 Å), $\text{B}_2\text{-H}_5$, $\text{B}_2\text{-H}_6$, $\text{B}_2\text{-H}_7$, $\text{B}_2\text{-H}_8$ (1.220 Å), $\text{B}_1\text{-Be}$ (1.918 Å), and $\text{B}_2\text{-Be}$, $\text{B}_2'\text{-Be}$ (2.001 Å). Coordinates for the monomeric solid-state fragment are given in Table I. Coordinates for longer chain lengths can be generated from those of Table I by successive 90° rotations about the Z axis, followed by a positive shift in Z of 4.2992 au. In addition, a single calculation on the supposed gas-phase structure of D_{2d} symmetry was performed for comparison to the solid-state structure. The D_{2d} gas-phase structure was chosen for this purpose because the coordination about beryllium in this structure (double hydrogen bridges) most closely resembles that of the solid-state configuration. Coordinates for this calculation were the same as used previously.¹

Localized orbitals for each fragment were obtained by maximizing the sum of the squares of displacements of the orbital centroids from an arbitrarily defined molecular origin. This is the well-known criterion of Boys,¹⁵ as implemented by the Edmiston-Ruedenberg¹⁶ procedure.

Results and Discussion

For reference, we compare all computed properties of the polymeric chains to those of the unstrained, linear structure

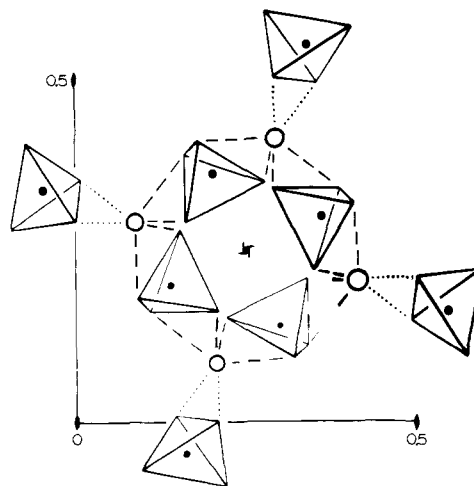


Figure 2. Portion of the unit cell, showing one helical polymeric chain around a 4_1 axis and projected along the c axis. Hydrogen arrangements are approximately tetrahedral around B (●) and trigonal prismatic around Be (○).

Table I. Coordinates of the Asymmetric Unit of Solid-State Beryllium Borohydride^a

atom	x	y	z
H ₁	-4.157 71	-8.389 45	1.105 81
H ₂	-0.788 56	-9.216 07	-0.736 22
H ₃	-1.005 88	-6.409 77	1.831 68
H ₄	-2.830 40	-6.076 87	-1.559 73
H ₅	-3.814 97	-2.513 11	0.254 95
H ₆	-0.781 29	-2.382 41	2.389 97
H ₇	-2.680 90	0.814 20	1.702 89
H ₈	-4.165 46	-1.732 86	3.955 21
B ₁	-2.218 57	-7.698 28	0.154 77
B ₂	-2.867 32	-1.454 16	2.070 41
Be	-1.292 02	-4.197 89	0.000 00

^a Atomic units.

with D_{2d} symmetry and double hydrogen bridges between boron and beryllium atoms. This structure, although not necessarily the lowest energy conformer in the gas phase, most closely resembles the structure found in the solid state. In adopting the "supermolecule" approach to modeling the solid-state structure, we of course are considering only effects within each helix, and not any interhelical interactions. This approximation seems reasonable, since the shortest interhelical H-H and B-B contacts are 2.73 and 3.74 Å, respectively.

For each polymeric fragment $(\text{BeB}_2\text{H}_8)_n$, the electronic structure of the central BeB_2H_8 moiety (or the central two moieties for even-numbered n) will most closely approximate that of the infinite chain length limit. Therefore, the computed properties discussed below (with the exception of total energy) are those calculated for the central BeB_2H_8 unit in the chain, or, in the case of even n , the average of the properties of the two central units.

Energetics. Total energies and virial ratios for the six solid-state fragments and the D_{2d} structure are given in Table II. A clear trend is evident in the virial ratios of the solid-state fragments. The longer the chain length, the closer the virial ratio is to unity. Each polymeric fragment is bound relative to the free atoms. In Figure 3, we present a plot of ΔE vs. chain length, where ΔE represents the energy change for the growth of the chain by one monomeric unit:

$$(\text{BeB}_2\text{H}_8)_{n-1} + (\text{BeB}_2\text{H}_8)_{D_{2d}} \rightarrow (\text{BeB}_2\text{H}_8)_n$$

$$\Delta E_n = E(\text{BeB}_2\text{H}_8)_n - E(\text{BeB}_2\text{H}_8)_{n-1} - E(\text{BeB}_2\text{H}_8)_{D_{2d}}$$

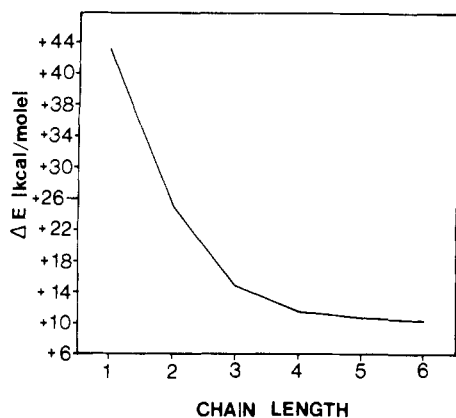


Figure 3. Plot of ΔE_n vs. n for the beryllium borohydride polymer (see text).

Table II. Total Energies for $(\text{BeB}_2\text{H}_8)_n$ Fragments

n	E^a	$-E/T$
1	-68.4381	0.9960
2	-136.9087	0.9964
3	-205.3957	0.9968
4	-273.8872	0.9969
5	-342.3801	0.9970
6	-410.8738	0.9971
D_{2d}	-68.5089	0.9984

^a Atomic units.

Here the reference gas-phase structure is assumed to be of D_{2d} symmetry. We note that the value of ΔE_1 (+44.4 kcal/mol) represents the energy necessary to distort the gas-phase D_{2d} structure to the solid-state geometry. This involves changing the B-Be-B bond angle from 180 to 124.8° and concurrent but smaller changes in all other bond lengths and angles. While each fragment from $n = 1$ to $n = 6$ is bound relative to the free atom energies, even the hexamer is not bound relative to six isolated D_{2d} monomers. Nevertheless, the rapid convergence of ΔE as a function of chain length indicates that we are near the infinite chain length limit for ΔE with this basis set at $n = 5$ or 6. The difference $\Delta E_5 - \Delta E_6$ is only 0.5 kcal/mol. Taking ΔE_6 as the infinite chain length limit, we find a 44% error for ΔE_3 , a 14% error for ΔE_4 , and a 5% error for ΔE_5 . The instability of the polymeric units relative to the D_{2d} monomers is almost certainly due to the well-known underestimation of bridge hydrogen stability by a minimum basis set.¹⁷ For instance, minimum basis set calculations yield¹⁷ a calculated ΔE for the dimerization of borane of -7.3 kcal/mol compared to the most probable experimental value¹⁸ of -34.9 kcal/mol. This error is due partially to a lack of polarization functions in the basis set (~12 kcal/mol error) and partially to neglect of electron correlation (~16 kcal/mol error).¹⁹ Thus, the high values for ΔE_n are probably associated with the fact that condensation of beryllium borohydride from the D_{2d} structure to the polymer involves the formation of two new Be-H-B interactions. Assumption of a modest minimum basis set error of 5 kcal/mol per Be-H-B interaction (only 36% of the error found in diborane) will make ΔE_6 negative. In fact, the minimum basis set error is probably substantially larger than 5 kcal/mol. Of course, other effects not considered here, such as interhelical electrostatic interactions, may well stabilize the crystalline phase. In addition, our ΔE values have been calculated relative to the D_{2d} gas-phase structure, which is not necessarily the actual lowest energy conformer in the gas phase (although it is the lowest energy structure within the minimum basis set approximation).¹

Inner shell eigenvalues for boron and beryllium, which are

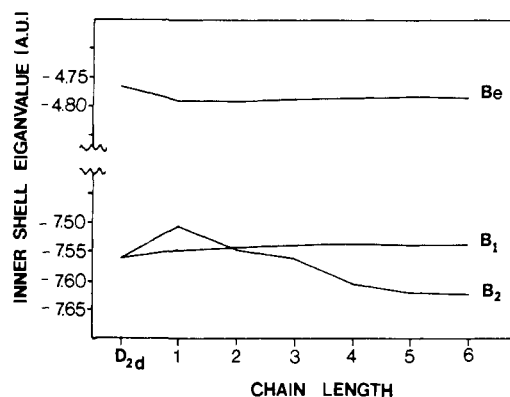
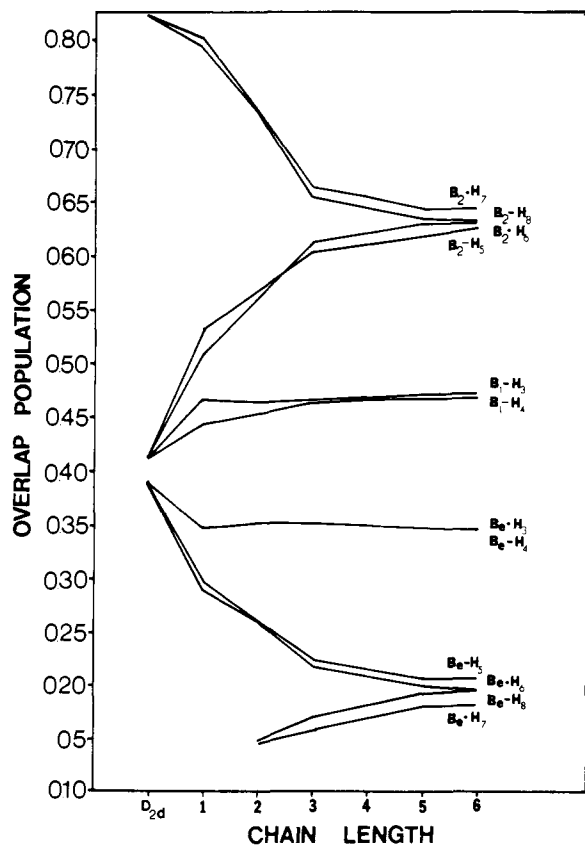
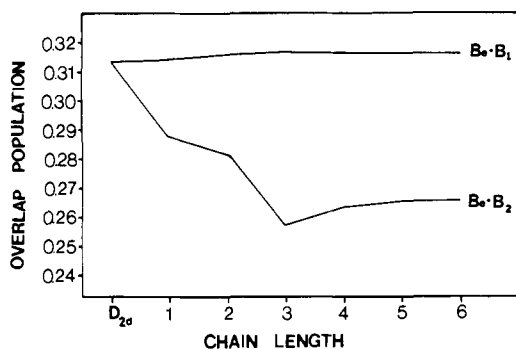


Figure 4. Plot of inner shell eigenvalues vs. n .

often used as a measure of molecular charge distribution, are plotted as a function of chain length in Figure 4. The values reported correspond to eigenvalues associated with the boron and beryllium atoms in the center of the polymeric fragment, averaged as described earlier for even-numbered fragments. Again, convergence is fair at the $n = 3$ level and very good at $n = 5$, the largest difference between $n = 5$ and $n = 6$ being 0.004 au (for B_2). Average errors relative to the hexamer are 0.0098 (trimer), 0.0059 (tetramer), and 0.0017 au (pentamer).

Overlap Populations. Overlap populations as a function of chain length for B-H and Be-H interactions are shown in Figure 5. Again, reasonable convergence is obtained at $n = 3$, but full convergence requires $n = 5$ or 6. Average errors are 0.016 (trimer), 0.009 (tetramer), and 0.002 (pentamer) relative to the hexamer. The results from the hexamer provide considerable information concerning the nature of the bonding in the solid state. In particular, the four strongest B-H bonding interactions fall into a narrow range of overlap population and correspond to the four B-H interactions within the helix. Similarly, the four Be-H interactions within the helix are grouped together and have the lowest overlap populations in the chemical repeat, substantially lower than the Be-H overlap populations external to the helix. These data strongly suggest that the interpretation of the solid-state structure as $\text{BeBH}_4^+ - \text{BH}_4^-$ (with the BH_4^- group within the helix) is substantially correct, although the small but still significant values of the Be-H overlap populations within the helix suggest that there is some covalent interaction between the ions. The Be-B overlap populations (Figure 6) support this conclusion. The Be-B₁ overlap population is greater than that of Be-B₂, implying a greater covalent interaction for Be-B₁, external to the helix. Average errors for BeB overlap populations (relative to the hexamer) are 0.020 (trimer), 0.003 (tetramer), and 0.000 (pentamer).

Mulliken Charges. Figure 7 illustrates Mulliken atomic charges for the central atoms of each polymeric fragment as a function of chain length. To the extent that the computed charges measure the actual distribution of charge in the molecule, the general trend is a lowering of (negative) charge on the hydrogens and an increase in charge on the borons and berylliums relative to the gas-phase monomer. The overall ordering of charges does not remain constant until $n = 5$; however, the absolute errors relative to the hexamer are modest for the trimer (0.01 e) and very small for the tetramer (0.003 e) and the pentamer (0.002 e). The two most negative hydrogens, H₁ and H₂, are the only two terminal hydrogens in the chemical repeat. It is well known²⁰ that bridging hydrogens tend to have more positive Mulliken charges than terminal hydrogens, and that trend is clearly reflected here. Charges for B_2 are clearly more negative than those for B_1 in each fragment, suggesting that an ionic description of the solid

Figure 5. Plot of B-H and Be-H overlap populations vs. n .Figure 6. Plot of Be-B overlap populations vs. n .

might involve a BH_4^- group including B_2 , but inner-shell eigenvalues (Figure 4), which are ordered $\text{B}_1 > \text{B}_2$, suggest the opposite trend (large inner-shell eigenvalues implying high negative charge).

Localized Orbitals. For each fragment, localized orbitals were calculated by procedures described previously.²¹ In every case, the localization calculation converged quickly to well-localized two- and three-centered orbitals (inner shells were excluded from the localizations). The bonding patterns in the chemical repeat consist of two-center B-H orbitals ($\text{B}_1\text{-H}_1$ and $\text{B}_1\text{-H}_2$) and six three-center Be-H-B orbitals ($\text{Be-H}_3\text{-B}_1$, $\text{Be-H}_4\text{-B}_1$, $\text{Be-H}_5\text{-B}_2$, $\text{Be-H}_6\text{-B}_2$, $\text{Be-H}_7\text{-B}_2'$, and $\text{Be-H}_8\text{-B}_2'$). Considering the center of the $n = 6$ fragment, the four Be-H-B orbitals within the helix are very asymmetrical, with average atomic contributions from beryllium, hydrogen, and boron of 0.24, 0.99, and 0.79 e, respectively. Conversely, the Be-H-B orbitals external to the helix are considerably more symmetrical. Average beryllium, hydrogen, and boron atomic populations for these orbitals are 0.40, 1.03, and 0.60 e, respectively. These data again support the idea that the solid

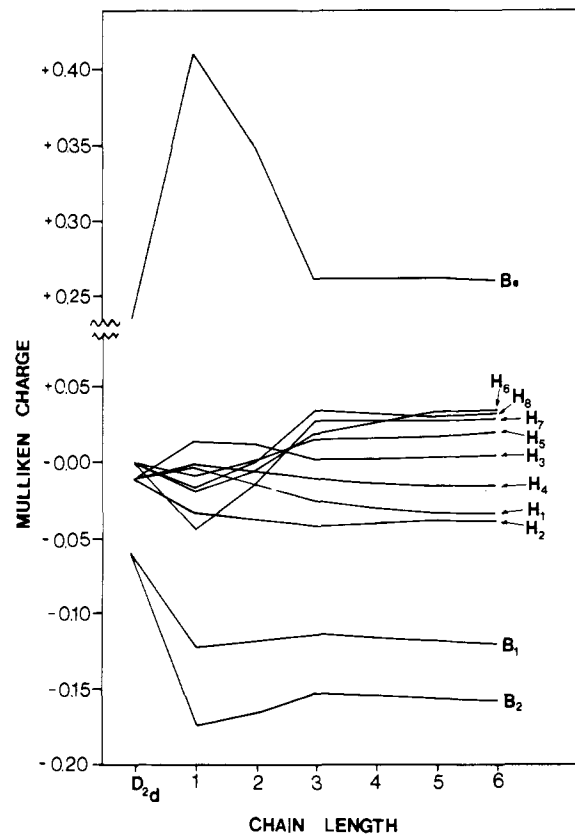
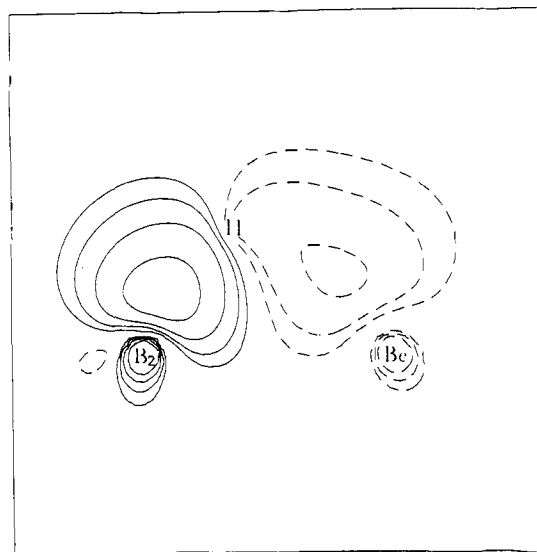
Figure 7. Plot of Mulliken charges vs. n .

Figure 8. Difference electron density map between a Be-H-B interaction within the helix and one of the D_{2d} monomer (see text). The contour levels are ± 0.002 , ± 0.004 , ± 0.008 , and ± 0.016 e/au³. Dashed lines indicate negative values.

may be viewed as $\text{BeBH}_4^+ \text{-} \text{BH}_4^-$, with small covalent interactions between the ions.

Truncation of the small nonlocal contributions to each localized orbital and subsequent renormalization allow an estimation of percent s character in each hybrid, and thus calculation of degrees of hybridization. Average values for the central BeB_2H_8 units of the hexamer are $sp^{2.1}$ for beryllium, $sp^{4.7}$ for the boron external to the helix, and $sp^{3.0}$ for the boron within the helix. Once again, the exact tetrahedral hybridization about the boron atom within the helix is suggestive of BH_4^- .

Electron Density. For a direct comparison of electron density in the monomer and polymeric fragments, we have computed two electron density maps, one being the central Be–H–B localized orbital of the trimer and the other being the Be–H–B localized orbital of the D_{2d} monomer, but with bond lengths constrained to equal those of the solid state. The trimer was chosen for computational convenience and because all indications are that electron reorganization upon going from the inner part of the trimer to the inner part of the hexamer is small compared to that from the monomer to the trimer (e.g., see Figures 5–7). The distortion of the monomeric D_{2d} bond lengths to those of the solid state allows a direct measure of reorganization of electron density brought about solely by BeB_2H_8 units bonding to each end of the monomer, and not by bond-length changes. In Figure 8, we show a difference electron density map calculated as

$$\rho_{\text{diff}} = \rho_{\text{trimer}} - \rho_{D_{2d}}$$

for the central Be–H–B localized orbital within the helix. The pronounced “flow” of electron density from the region of the beryllium to the region of the boron is another strong indication of the increased ionic character of the Be–B interaction within the helix.

Conclusion

Overlap populations, localized orbitals, and electron density comparisons all indicate that solid-state beryllium borohydride is best viewed as $\text{BeBH}_4^{\delta+}-\text{BH}_4^{\delta-}$, with the boron–beryllium interaction within the helix clearly being more ionic than in the D_{2d} monomer. This conclusion is consistent with the known geometrical parameters of the solid state⁶ and the infrared spectrum of the solid.⁷

Calculated properties of the molecular wave function for the central region of the polymeric fragments show little difference between the pentamer and the hexamer. Therefore, it seems reasonable to conclude that the hexamer results are close to the limit of infinite chain length. Properties calculated from

the center BeB_2H_8 unit of the trimer agree only moderately well with those calculated from the hexamer, but virtually all of the inaccuracies associated with the trimer properties are corrected at the pentamer level. The pentamer corresponds to two BeB_2H_8 units on each end of the central BeB_2H_8 moiety, and the above results indicate that two monomeric units are necessary to eliminate edge effects in modeling the solid-state polymer.

Acknowledgments. This work was partially supported by the Robert A. Welch Foundation.

References and Notes

- (1) D. S. Marynick and W. N. Lipscomb, *J. Am. Chem. Soc.*, **95**, 7244 (1973).
- (2) R. Ahlrich, *Chem. Phys. Lett.*, **19**, 174 (1973).
- (3) D. S. Marynick, *J. Chem. Phys.*, **64**, 3080 (1976).
- (4) M. J. S. Dewar and H. S. Rzepa, *J. Am. Chem. Soc.*, **100**, 777 (1978).
- (5) (a) J. W. Nibler, *J. Am. Chem. Soc.*, **94**, 3349 (1972); (b) G. Gundersen, L. Hedberg, and K. Hedberg, *J. Chem. Phys.*, **59**, 3777 (1973).
- (6) (a) D. S. Marynick and W. N. Lipscomb, *Inorg. Chem.*, **11**, 820 (1972); (b) *J. Am. Chem. Soc.*, **93**, 2322 (1971).
- (7) J. W. Nibler, D. F. Shriver, and T. H. Cook, *J. Chem. Phys.*, **54**, 5257 (1971).
- (8) A. B. Burg and H. I. Schlesinger, *J. Am. Chem. Soc.*, **62**, 3425 (1940).
- (9) (a) J. W. Nibler and J. McNabb, *Chem. Commun.*, 134 (1969); (b) J. W. Nibler and T. Dyke, *J. Am. Chem. Soc.*, **92**, 2920 (1970).
- (10) T. A. Halgren and W. N. Lipscomb, *J. Chem. Phys.*, **58**, 1596 (1973).
- (11) C. E. Dykstra, H. F. Schaefer, and W. Meyer, *J. Chem. Phys.*, **65**, 5141 (1976), and references cited therein.
- (12) T. A. Halgren, D. A. Kleier, J. H. Hall Jr., L. D. Brown, and W. N. Lipscomb, *J. Am. Chem. Soc.*, **100**, 6595 (1978).
- (13) W. J. Hehre, R. F. Stewart, and J. A. Pople, *J. Chem. Phys.*, **51**, 2657 (1969).
- (14) T. A. Halgren, R. J. Anderson, D. S. Jones, and W. N. Lipscomb, *Chem. Phys. Lett.*, **8**, 547 (1971).
- (15) J. M. Foster and S. F. Boys, *Rev. Mod. Phys.*, **32**, 300 (1960).
- (16) C. Edmiston and K. Ruedenberg, *Rev. Mod. Phys.*, **35**, 457 (1963).
- (17) D. A. Dixon, I. M. Pepperberg, and W. N. Lipscomb, *J. Am. Chem. Soc.*, **96**, 1325 (1974).
- (18) G. W. Mappes, S. A. Friedman, and T. P. Fehlner, *J. Phys. Chem.*, **74**, 3307 (1970).
- (19) D. S. Marynick, J. H. Hall Jr., and W. N. Lipscomb, *J. Chem. Phys.*, **61**, 5460 (1975).
- (20) I. R. Epstein, J. A. Tossell, E. Switkes, R. M. Stevens, and W. N. Lipscomb, *Inorg. Chem.*, **10**, 171 (1971).
- (21) D. A. Kleier, T. A. Halgren, J. H. Hall Jr., and W. N. Lipscomb, *J. Chem. Phys.*, **61**, 3905 (1974).

X-ray Photoemission Study of Platinum Carbonyl Dianions $[\text{Pt}_3(\text{CO})_6]_n^{2-}$ ($n = 2, 3, 4, 5, 6, \sim 10$)

G. Apai,* S.-T. Lee, M. G. Mason, L. J. Gerenser, and S. A. Gardner

Contribution from the Research Laboratories, Eastman Kodak Company, Rochester, New York 14650. Received May 7, 1979

Abstract: A series of platinum carbonyl dianion clusters has been studied by X-ray photoemission spectroscopy. Members of the series include $[\text{Pt}_3(\text{CO})_6]_n^{2-}$ where $n = 2, 3, 4, 5, 6, \sim 10$. The general structure of all valence spectra, in particular that of the Pt 5d derived bands, is remarkably similar. This observation is taken to be evidence that negligible interaction exists between the $\text{Pt}_3(\text{CO})_6$ layers. We observe changes in the binding energies of Pt 4f, Pt 4d, and the molecular orbitals ($5\sigma + 1\pi$) of the carbonyl ligands as a function of cluster size. All levels except the carbonyl 4s orbitals are shifted to higher binding energy asymptotically as the cluster size increases. This behavior of binding energies is interpreted as being due to the decreasing effect of the anion charge in larger clusters and to the bonding character of the ($5\sigma + 1\pi$) orbitals.

Introduction

Metal cluster chemistry has become an additional way for surface-physics research to understand chemisorption of molecules on transition-metal surfaces. Recently, several papers have commented on the analogy which exists between transition-metal cluster complexes and few-atom bare metal

clusters.¹ We and others feel that cluster complexes may provide a way of studying metal–metal and metal–adsorbate interactions in a more straightforward way than with metals themselves.

We have chosen to study platinum carbonyl dianion oligomers by X-ray photoemission spectroscopy (XPS) for several